Hindawi
Journal of Nanomaterials
Volume 2022, Article ID 3668458, 11 pages
https://doi.org/10.1155/2022/3668458

Research Article

Investigation on the Performance of Domestic Refrigerator with Zirconium Oxide-R134a Nanorefrigerant

A. Baskaran,[1] **N. Manikandan**,[2] **JuleLeta Tesfaye**,[2,3] **N. Nagaprasad**,[4] **and R. Krishnaraj**[3,5]

[1]*Department of Mechanical Engineering, P.A. College of Engineering and Technology, Pollachi, 642002 Tamilnadu, India*
[2]*Department of Physics, College of Natural and Computational Science, Dambi Dollo University, Ethiopia*
[3]*Centre for Excellence-Indigenous Knowledge, Innovative Technology Transfer and Entrepreneurship, Dambi Dollo University, Ethiopia*
[4]*Department of Mechanical Engineering, ULTRA College of Engineering and Technology, Madurai, 625104 Tamilnadu, India*
[5]*Department of Mechanical Engineering, College of Engineering and Technology, Dambi Dollo University, Ethiopia*

Correspondence should be addressed to R. Krishnaraj; prof.dr.krishnaraj@dadu.edu.et

Received 20 July 2021; Revised 11 November 2021; Accepted 28 February 2022; Published 18 March 2022

Academic Editor: Zafar Iqbal

This study investigates the performance of nanorefrigerants (R134a-ZrO_2) in a domestic refrigerator at a concentration of 0.2 g/l without changing the components. Nanoparticles of ZrO_2 of 0.2 g/L concentration with particle size 1-10 nm and 140 g of R134a have been charged, and investigations were carried out. Energy consumption and pull-down tests were conducted to investigate the performance of the refrigerator. The performance parameters like refrigeration capacity, compressor power, discharge temperature, coefficient of performance, and energy consumption were investigated for the nanorefrigerant (R134a-ZrO_2), and the results were compared with base refrigerant R134a. The pull downtime, energy consumption, and discharge temperature are reduced with increased COP and compressor power when the system is operated with R134a-ZrO_2 nanorefrigerant. Also, the thermophysical properties of the nanorefrigerant (R134a-ZrO_2) are calculated and analyzed for the various volume fraction of nanoparticles.

1. Introduction

In this present scenario, nanoparticles and nanofluids have attracted attention from several research works. Nanoparticles are in the order of 15-nanometer particles. Nanofluids are designed colloids consisting of a primary fluid suspended from nanosize particles (1-15 nm). Nanofluids have the special advantage of having enhanced characteristics as compared to base fluids. They have many attractive characteristics, such as improving thermal physical properties, higher thermal conductivity, and higher surface area. Metal oxides, carbides, nitrides, carbon nanotubes, diamonds, and other nanoparticles may be dispersed in base fluids. Given the higher thermal conductivity of solids than fluids, it was first proposed by Maxwell [1] to disperse metal particles into fields to improve fluid thermal conductivity. Earlier studies have used solid particles with various sizes have subject to major problems such as clogging tendencies, erosion, surface abrasion, and high-pressure decreases. The use of nanofluids ensures that these problems can be overcome. Choi and Eastman [2] measured thermal conductivity of 13 nm Al_2O_3–water and 27 nm TiO_2–water. It was observed that when 4.3 percent of the volume fractions of Al_2O_3 and TiO_2 nanoparticles were incorporated in water, the thermal fluid conductivity increased in comparison to pure water by 32% and 11%, respectively. This is the first report on nanopowder and was the basis of further thermal fluid conductivity studies. In order to improve conductivity, they have been introduced the concept by mixing 1-15 nm large nanoparticles into liquids and called nanofluids. This concept has been extended to refrigerants in recent times. The development of nanofluids is aimed at increasing the thermal flow performance of different heat transfer fluids.

The performance of the cooling system with Al_2O_3-PAG oil was researched by Kumar and Elansezhian [3]. The performance of the cooling system was better than the pure lubricant of working fluid R134a, and energy consumption was reduced by 10.32% at 0.2% volumetric. The results show that the coefficient of heat transfer increases with nano-Al_2O_3. Therefore, it is found possible to use Al_2O_3 nanorefrigerant in the cooling system. Sreejith [4] studied the performance of the refrigerator with air and a water-cooled condenser with a 0.06 percent mass fraction of CuO mixture and various compressor oils. Compared with the HFC134a/POE oil system and between 9 and 14% while using a water-cooled condenser under various load conditions, the energy consumption was reduced between 12% and 19% with SUNISO 3GS mineral oil system. The performance of domestic refrigerators with different nanorefrigerants was studied by Subramani et al. [5]. Desai and Patil [6] conducted an experiment to investigate the performance of a refrigerator compressor in which SiO_2 nano-oil is offered as a viable lubricant. Energy consumption tests were used to assess the VCRS performance using nanoparticles. When nano-oil was utilized instead of pure oil, the COP of the system was improved. An experimental investigation was performed by Kushwaha et al. [7] on a nanorefrigerant (R134a+Al_2O_3)-based refrigeration system. The results indicate that the coefficient of performance increases with the usage of nano-Al_2O_3. Veera et al. [8] experimented with nanorefrigerants (Al_2O_3-ethylene glycol oil and TiO_2-ethylene glycol oil) in an R134a vapour compression refrigeration system. The system was subjected to a cooling capacity test. The results show that using nano-Al_2O_3 and TiO_2 increases the heat transfer coefficient. Thus, it has been discovered that using Al_2O_3 and TiO_2 nanorefrigerants in refrigeration systems is feasible.

Haque et al. [9] studied the performance of a household refrigerator by the addition of nanoparticles into this lubricant. The polyester (POE) oil has been added at two different volume concentrations to different sizes of nanoparticles of Al_2O_3 and TiO_2 (0.05 and 0.1%). The refrigerator is tested for energy consumption and freezer capacity. Kumar et al. [10] investigated the performance of a VCRS with ZrO_2 nanoparticle in the working liquid. The concentration of nano-ZrO_2 with the particle size of 20 nm ranging from 0.01% to 0.06% with R134a and R152a is studied. Krishnan et al. [11] analyzed the performance of nanocoolant (Al_2O_3–R290/R600a) in a VCRS. The simulation programme based on the stable state mathematical models of the VCR system performed this analysis. The results show that the coefficient of performance, mass flow rate, and actual compressor piston displacement is heavier while heat rejection and compressor power are slightly lower in the nanocoolant mix. Baskar and Karikalan [12] did the study to increase the functioning of a vapour compression cooler compressor, and ZrO_2 nano-oil was used as a potential lubricant. The usage of nano-oil with precise concentrations of 0.1%, 0.2%, and 0.3% was added to the compressor oil (by a mass fraction). The study demonstrates that using nano-oil instead of pure oil enhanced the system's COP by 7.61 percent, 14.05 percent, and 11.90 percent, respectively. Singh and Ansari [13] present experimental work on the cooling system using nanorefrigerant (R600a/R290). This cooling system was made up of three different volumetric (0.15, 0.25, and 35 g) concentrations of CuO particles of size (20-30 nm). An improved performance coefficient was also observed during the study (3.18%-11.57%). Jatinder et al. [14] study the energetic and energetic behaviours of a household cooler using several lubricants, such as R134a and LPG coolants, polyol-ester, mineral oils (MO), and TiO_2, SiO_2, and Al_2O_3 nanoparticles distributed in mineral oil. The refrigerator with a 40 g charge of LPG/TiO_2–MO lubrication (0.2 g/L TiO_2) had the highest COP efficiency and 2nd efficiency, with the minimum compressor energy usage and 100% irreversibility. Adelekan et al. [15] present an experimental analysis of energy consumption and heat transmission performance of the safe mass charge of LPG refrigerant by enhanced nanoparticles 0.2 g/l, 0.4 g/l, and 0.6 g/l in a home refrigerator with varying concentrations. All nanolubricants based on TiO_2 have been observed to reduce average power consumption. Baskaran et al. [16–27] evaluated the performance of a vapour compression refrigeration device using a variety of different refrigerants (including refrigerant mixtures) and nanorefrigerants, and their findings were compared to those obtained by using R134a as a potential alternative replacement. An investigative test rig is indigenously created and manufactured to conduct the examinations. The system effectiveness was evaluated with and without nanoparticles. Several studies have been conducted to address the problem of global warming and the depletion of the ozone layer using alternative refrigerants in the refrigeration system, therefore considered to be a useful attempt to study the effect of a surfactant and examine detailed possibilities of exploring a new alternative refrigerant and incorporating nanoparticles into the refrigerant.

Shaheed [28] studied the surface tension of nanofluids which increases with increasing particle concentration but decreases with increasing temperature. The density of nanofluids increases with the increasing volume concentration of nanoparticles and decreases with increasing temperature. Specific heat of nanofluids increases with increasing temperature and volume concentration. Comparison of various nanorefrigerants for the performance enhancement of VCRS are listed in Table 1.

Imaduddin [29] used the refrigerant R134a and POE oil (300 ml) suspended with TiO_2 nanoparticles (2.5 g). The author found that the COP increased by 22.5 percent when compared to R134a VCRS without nanoparticle. Kumar et al. [30] tested the VCRS performance using refrigerant R134a and PAG oil (150, 180, and 200 ml) suspended with Al_2O_3 nanoparticles (0.2 percent concentration by volume) and found that the COP increased by 3.5 percent. At the same time, the power consumption decreased by 10.32 percent compared to R134a VCRS without nanoparticle. Various experimental analyses were conducted to study the performance of VCR system with nanorefrigerants which reveals the enhancement of performance.

In today's scenario, air conditioning and refrigeration are essential equipment for people's comfort. The researchers are focused on increasing cooling capacity and developing a

Table 1: Comparison of various nanorefrigerants for the performance enhancement of VCRS.

Author	Ref system	Ref. type	Oil in compressor	Nanoparticles			Test rig	COP	System power consumption
				Type	Concentration	Weight in g per ml of oil			
Syed Shaheed [28]	VCRS	CARE 30		Al_2O_3 TiO_2					
Shaik Imaduddin [29]	VCRS	R134a	POE	TiO_2		2.5 g/350 ml	YES	22.5% higher	
Sendil Kumar et al. [30]	VCRS	R134a	PAG (poly alkylene glycol)	Al_2O_3	0.2%V	PAG-150 ml, 180 ml, and 200 ml	YES	3.5	10.32% reduced
Fadhilah et al. [31]	Copper tube of an evaporator coil	R134a		CuO	1%V				
Coumaressin et al. [32]	VCRS	R134a		CuO	0.05 to 1%		YES		
Sanukrishna et al. [33]	VCRS	R134a	PAG (poly alkylene glycol)	CuO	0.06%, 0.08%, 0.1% by volume		Yes		
Sendil Kumar et al. [34]	VCRS	R152a		ZnO	0.1%V, 0.3%V, 0.5%V		Yes		21% less@0.5%V
Present study	VCRS		PAG (poly alkylene glycol)	ZrO_2		0.2 g/L	Yes	2.1% higher	Energy consumption is reduced by 6.25% Refrigeration capacity increased by 38.7%% Pull downtime decreased by 23.3%

(a) (b)

Figure 1: Zirconium oxide. (a) Zirconium oxide nanoparticle; (b) SEM image of zirconium oxide.

cooling system that is energy efficient. Nanotechnological goods, methods, and applications contribute to environmental and climate conservation by conserving raw materials, energy, and water, as well as lowering greenhouse gas emissions and hazardous waste. Nanoparticles improve the thermal, chemical, and other properties of the refrigerant in the refrigeration system. The use of nanorefrigerants in small amount in vapour compression refrigeration system aided in improving system performance. This paper examines the thermophysical properties of nanorefrigerant (R134a-ZrO_2) and the thermal performance of the system used in a residential refrigerator.

2. Materials and Methods

2.1. Zirconium Dioxide (ZrO_2) Nanoparticles. Polyvinyl pyrrolidone was employed as the capping agent, and deionized water was utilized as the solvent in the thermal treatment technique, which used zirconium (IV) acetate hydroxide to produce zirconium dioxide nanoparticles with monoclinic composition as a substrate and deionized water as the solvent. It was necessary to combine the chemicals and eliminate them in accordance to generate a standardised solution, which was then immediately calcinated in order to create the pure nanocrystalline powder that was validated by the results of the FTIR, EDX, and SEM tests. Thermal calcination at temperatures ranging from 600 to 900 degrees Celsius allowed for precise control of the dimensions and optical characteristics of nanoparticles. It was discovered by XRD and transmission electron microscope images that the mean particle sizes grew larger as the calcination temperature rises. The optical characteristics of the material were investigated using a UV-Vis spectrophotometer, which revealed that the bandgap energy decreased as the calcination temperature increased. UV-Vis absorption spectroscopy is a nondestructive technique for determining the optical characteristics of semiconductor nanostructures. By dissolving the nanopowder in ethanol in the wavelength range of 700 nm to 200 nm, the absorption spectra of samples were recorded using a JASCO V-670 UV-Vis absorption spectrophotometer. These results show that size-controlled zirconium nanoparticles with reduced time and energy consumption of the synthesis were manufactured in a convenient way with the elimination of the drying method (24 h) in the current thermal treatment technique. Figure 1 illustrates the SEM image of zirconium oxide, and Table 2 shows the properties of zirconium oxide.

Table 2: Properties of zirconium oxide.

Chemical composition (%)	Zirconium	74.03
	Oxygen	24.34
Physical properties	Density	5680 kg/m^3
	Molar mass	231.891 g/mol
Thermal properties	Melting point	2715°C
	Boiling point	4300°C

2.2. Thermophysical Properties of Nanofluid. Thermophysical parameters of nanofluids are extremely important in predicting their heat transfer behaviour. It is critical in terms of industrial and energy-saving control. Nanofluids have sparked the interest of the industry. When compared to traditional particles such as fluid suspension, millimetre, and micrometre-sized particles, nanoparticles have a lot of potentials to improve thermal transport qualities. The transport properties of nanofluid are influenced by a variety of elements, including particle volume fraction, particle material, particle size, particle shape, base fluid material, temperature, mixture combinations, slide mechanisms, and surfactant. When compared to a base fluid, studies have shown that using nanofluid increases both thermal conductivity and viscosity.

2.3. Thermal Conductivity. To model the thermal conductivity of nanofluid, a variety of experimental and theoretical researches have been undertaken in the literature. The preceding results were mostly based on the definition of a two-component mixture's effective thermal conductivity. One of the first models developed for solid-liquid mixtures with relatively sizable particles was Maxwell [1] model. It was based on a solution of the heat conduction equation.

The effective thermal conductivity (Equation (1)) is given by

$$(K_{\mathrm{eff}}) = K_{\mathrm{bf}} \frac{K_p + 2K_{\mathrm{bf}} + 2\Phi(K_p - K_{\mathrm{bf}})}{K_p + 2K_{\mathrm{bf}} - \Phi(K_p - K_{\mathrm{bf}})}, \quad (1)$$

where k_p is the thermal conductivity of the particles, k_{eff} is the effective thermal conductivity of nanofluid, k_{bf} is the base fluid thermal conductivity, and Φ is the volume fraction of the suspended particles.

The thermal conductivity of nanofluids rises with decreasing particle size, according to the experimental evidence. Two processes of thermal conductivity enhancement are theoretically suggested by this trend: Brownian motion of nanoparticles and liquid layering around nanoparticles (Ozerinc et al. [35]).

2.4. Viscosity. Researchers have utilized various viscosity models to model the effective viscosity of nanofluid as a function of volume fraction. Using empirical hydrodynamic equations, Einstein [36] calculated the effective viscosity of a suspension of spherical solids as a function of volume fraction (volume concentration less than 5%) (Equation (2)).

This equation was expressed by the following:

$$\mu_{\mathrm{eff}} = (1 + 2.5\phi)\mu_{\mathrm{bf}}, \quad (2)$$

where μ_{eff} is the effective viscosity of nanofluid, μ_{bf} is the base fluid viscosity, and ϕ is the volume fraction of the suspended particles.

Brinkman [37] proposed a viscosity correlation (Equation (3)) that extended Einstein's equation to suspensions with a moderate particle volume fraction, usually less than 4%.

$$\mu_{\mathrm{eff}} = \mu_{\mathrm{bf}} \frac{1}{(1-\phi)^{2.5}}. \quad (3)$$

Batchelor [38] investigated the influence of Brownian motion on the effective viscosity in a suspension of stiff spherical particles. The effective viscosity of an isotropic suspension was calculated using Equation (4).

$$\mu_{\mathrm{eff}} = (1 + 2.5\phi + 6.2\phi)\mu_{\mathrm{bf}}. \quad (4)$$

2.5. Specific Heat and Density. The specific heat capacity (Pak and Cho [39]) and density (Xuan and Roetzel [40]) of the nanofluid as a function of particle volume concentration and individual properties can be computed using the following equations (Equations (5) and (6)), respectively, using classical formulas derived for a two-phase mixture:

$$\rho_{\mathrm{eff}} = (1-\phi)\rho_{\mathrm{bf}} + \phi\rho_p, \quad (5)$$

$$\left(\rho_{\mathrm{cp}}\right)_{\mathrm{eff}} = (1-\phi)\left(\rho_{\mathrm{cp}}\right)_{\mathrm{bf}} + \phi\left(\rho_{\mathrm{cp}}\right)_p, \quad (6)$$

Figure 2: Photographic view of the experimental setup.

where ρ_{eff} is the effective density and ρ_{cp} is the specific heat capacity.

2.6. Experimental Setup. Figure 2 illustrates the photographic view of the domestic refrigerator of Kelvinator made with 185-liter capacity with a testing facility designed to work with R134a. It is comprised of an evaporator, a wire meshes wind cooled condenser, and a reciprocating compressor that is hermetically sealed. A total of four pressure gauges have been mounted at the compressor air intake and outlet as well as the condenser outlet and the evaporator inlet. All these pressure gauges were fitted on a wooden panel to avoid vibration during testing. The thermocouple wire was linked to the thermocouple analyzer at all 10 of its locations, which was a first. A thermocouple analyzer is a device that reads the temperatures that have been measured. It was decided to install ten calibrated temperature sensors at the evaporator inlet and outlet, compressor intake and outlet, compressor outlet, and condenser inlet, as well as the freezer section and refrigerator cabin. Furthermore, the voltage and current that were spent were recorded. Additionally, the flow meter, which also has been connected to the tubing running between both the condenser and the capillary tube, was permanently attached to the wooden panel. All of the data was captured using digital storage equipment for the Human Machine Interface (HMI), which was set to record data periodically every 10 seconds. To check the quality of condensed liquid flow, a sight glass is provided.

An energy meter of the Select MFM384 model with a capability of 100-500 V was connected to the compressor in order to assess the power and electricity consumption. Service ports were built on the upper face of the compressor to allow for the charging and recovery of refrigerant while the compressor was in operation. Initially, the service port was used to facilitate the removal of moisture from the system. The device was cleaned with nitrogen gas in order to remove any air, contaminants, moisture, or other things that may have accumulated inside the system and could have negatively impacted its operation. The system was charged by using a charging system. The system was vacuumed with the assistance of just a vacuum pump to pressure with 30 millimetres of mercury. The layout of the measurement device that was employed in the research setup is depicted

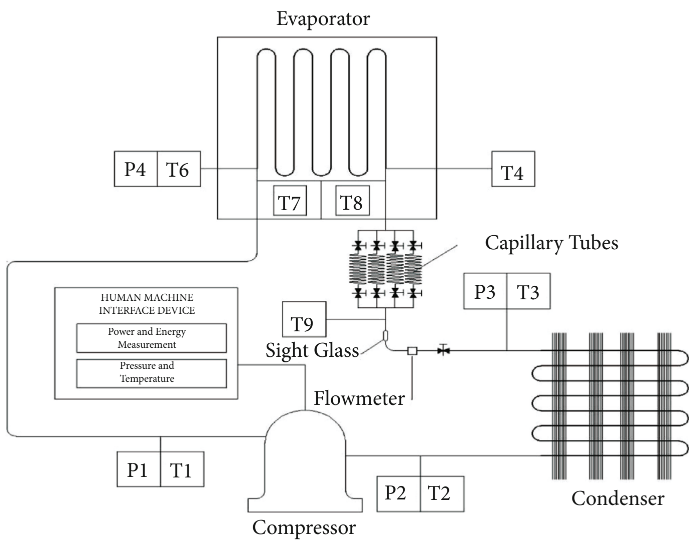

Figure 3: Schematic diagram of the measurement system in an experimental setup.

schematically in Figure 3. Table 3 lists the technical parameters of the residential refrigerator test unit, whereas Table 4 lists the measured quantities, as well as their range and precision, for the unit.

2.7. Uncertainty Analysis for Measuring Devices and Calculated Items

2.7.1. Temperature Measurement. RTD type sensors are used to measure the temperatures at various state points of the system. The maximum possible error in the case of temperature measurement is calculated from the minimum value of the thermocouple output and the accuracy of the instrument. The error in temperature measurement for thermocouples is

$$\frac{\partial t}{t} = \frac{0.1}{18} = 0.55\%. \quad (7)$$

2.7.2. Pressure Measurement. The pressure transducer is used to measure the pressure at various points in the system. The maximum error in the measurement of pressure for the condenser and evaporator side is

$$\frac{\partial P}{P} = \frac{0.1}{20} = \pm 0.5\%, \quad (8)$$

$$\frac{\partial P}{P} = \frac{0.1}{220} = \pm 0.04\%. \quad (9)$$

2.7.3. Flow Rate Measurement. A refrigerant flow meter was used to measure the refrigerant flow rate. The maximum error in the measurement of refrigerant flow rate is

$$\frac{\partial m}{m} = \frac{0.1}{100} = \pm 0.1\%. \quad (10)$$

Table 3: The technical characteristics of the residential refrigerator test unit.

Details	Specifications
Storage volume	169 L
Current rating	1.1 max
Voltage	220-240 V
Frequency	50 Hz
No. of doors	1
Refrigerant type	R134a
Defrost system	Auto defrost
Refrigerant charged	0.140 kg
Capillary tube length	3.35 m
Capillary tube inner diameter	0.00078 m
Cooling capacity	182 W

Table 4: Quantities that have been evaluated, along with respective range and precision.

Quantity	Range	Accuracy
Temperature	-40°C to 110°C	+0.1°C
Power consumption	0 to 1000 W	1 W
Voltage	0 to 240 V	0.1 V
Current	0 to 10 A	0.1 A
Pressure	0 to 150 MPa	+0.7 kPa
Flow rate	0 to 100 cc/s	0.1 cc/s

2.7.4. Power Measurement. A multifunction meter was used to measure the power consumption by the compressor. The maximum error in the measurement of power is

$$\frac{\partial \mathrm{CP}}{\mathrm{CP}} = \frac{1}{1000} = \pm 0.1\%. \quad (11)$$

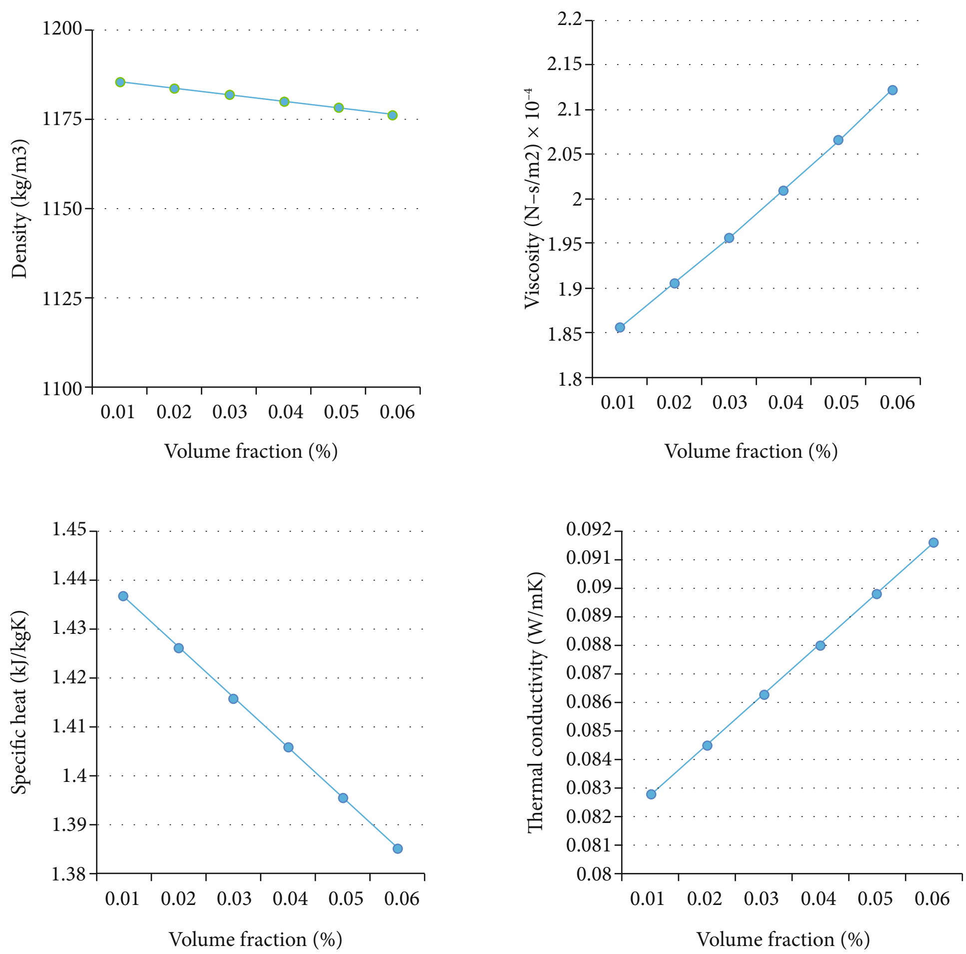

FIGURE 4: Variation of thermophysical properties of nanorefrigerant (R134a+ZrO_2) for various volume fraction of nanoparticle in %.

2.7.5. Refrigerating Capacity.

$$\frac{\partial RC}{RC} = \sqrt{\left(\frac{\partial m}{m}\right)^2 + 2\left(\frac{\partial T}{T}\right)^2} = \pm 0.784\%. \tag{12}$$

2.7.6. Coefficient of Performance.

$$\frac{\partial COP}{COP} = \sqrt{\left(\frac{\partial RC}{RC}\right)^2 + 2\left(\frac{\partial CP}{CP}\right)^2} = \pm 0.7903\%. \tag{13}$$

2.7.7. Test Procedure. As per the guidelines given by ASHRAE handbook, 2010, the energy consumption test and no-load pull-down test were conducted with the following system parameters.

Freezer compartment: -18°C to -15°C

Food compartment: 3°C to 5°C

Steady ambient temperature: 25°C to 32°C

Furthermore, certain randomized experiments were conducted to establish the reproducibility of the data. When the system was left to function, measurements were taken of the temperatures; pressure, energy consumed, and the amount of refrigerant flow were collected once in every ten seconds till the steady-state operating conditions were reached. The observed temperatures, pressures, mass flow rate, electric power, and energy were utilized to calculate the operation characteristics of the refrigeration system.

2.7.8. Pull Downtime. Generally speaking, pull downtime is described as the amount of time it takes to cool air within a refrigerator from its ambient temperature of 32 degrees Celsius to the ideal freezer and cabin air temperatures of 16 degrees Celsius and 4 degrees Celsius, respectively (ISO8187).

2.7.9. Refrigerating Capacity. Q_{eva} is the amount of cooling potential which may be represented as

$$Q_{eva} = m_r q_{eva}, \tag{14}$$

where m_r is the measured refrigerant mass flow rate and q_{eva} is the cooling effect of the evaporator.

2.7.10. Coefficient of Performance. The relationship between theoretical coefficients of effectiveness (COP_{th}) and real coefficients of performance (COP_{act}) could be represented as

$$COP_{th} = \frac{Q_{eva}}{P_{com}}, \tag{15}$$

$$\mathrm{COP_{act}} = \frac{Q_{eva}}{P_{elec}}, \tag{16}$$

where P_{elec} is the measured electric power supplied to the compressor and P_{com} is the theoretical power consumed by the compressor. P_{com} can be written as follows:

$$P_{com} = m_r w_{com}, \tag{17}$$

where w_{com} is the specific work of compressor, which is equal to the enthalpy difference through the compressor.

2.8. Experimental Analysis Procedure

2.8.1. Pull-Down Test. In this test, the cooling capacity of the system is evaluated. Refrigeration cycle off time will increase with the increase of cooling rate. During the test, doors were closed, and the refrigerator was under no-load condition. Temperatures at several places were measured every 10 seconds throughout the pull-down experiment until the temperature reached the targeted freezing threshold.

2.8.2. Compressor Energy Utilization, Cooling Effect, and Exact COP. The compressor energy consumption experiment is carried out at an ambient temperature of 32°C. Most assessments were made when the level of stability was attained. The energy usage of the energy meter was recorded. To calculate the actual COP and cooling effect, various freezer temperatures (-6°C to -16°C) were selected. At a particular freezer temperature, the observed mass flow rate and power are used to find COP and refrigerating effect.

3. Result and Discussions

3.1. Variation of Thermophysical Properties of Nanorefrigerant ZrO_2/R134a. The thermophysical properties of the ZrO_2/R134a nanorefrigerant are studied in relation to various volume fractions of nanoparticles. The thermal conductivity of ZrO_2/R134a nanorefrigerant increased with increasing particle concentration in this investigation. The improvement in thermal conductivity of nanorefrigerants is evident from experimental results. The increased surface area of nanoparticles and the Brownian motion of nanoparticles dispersed in the base fluid are responsible for the rise in conductivity.

Furthermore, the results of the nanorefrigerant's viscosity show a significant increase with increasing volume fractions, whereas specific heat and density change in the opposite direction. As a result, the optimal particle volume fraction of 0.02 percent is taken into account when producing nanorefrigerants that can improve the performance of the refrigeration system.

Figure 4 shows the variation of thermophysical properties of nanorefrigerant (R134a+ZrO_2) for various volume fractions of nanoparticles.

3.2. Pull Downtime. Figure 5 shows the plot of pull downtime for ZrO_2+R134a nanorefrigerant and pure R134a refrigerant. The pull downtime for nanorefrigerant at -14°C freezer temperature was reduced by 23.53% when compared

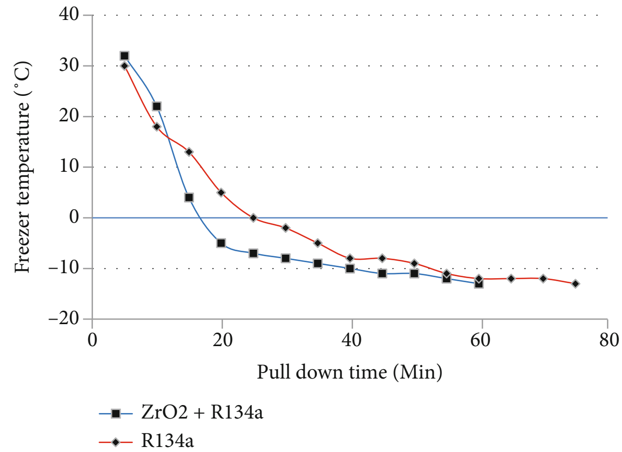

Figure 5: Variation of pull downtime for R134a and R134a+ZrO_2.

Table 5: Variation of evaporator inlet temperature with time.

Time (min)	Evaporator inlet temperature (°C)		Freezer temperature (°C)	
	R134a	R134a+ZrO_2	R134a	R134a+ZrO_2
0	29	31	30	32
5	6	-3	18	22
10	5	-5	13	4
15	3	-8	5	-5
20	-6	-10	0	-7
25	-8	-11	-2	-8
30	-10	-12	-6	-9
35	-11	-13	-8	-10
40	-12	-14	-8	-11
45	-12	-14	-9	-11
50	-13	-15	-11	-12
55	-14	-16	-12	-13
60	-14	-16	-12	-13
65	-14	-17	-12	-14
70	-15	-17	-13	-14
75	-15	-18	-13	-15
80	-15	-18	-13	-15
85	-15	-18	-14	-15
90	-16	-19	-14	-16
95	-16		-14	
100	-16		-14	

to pure R134a refrigerant. Table 5 indicates the variation of evaporator inlet temperature and freezer temperature with time.

3.3. Coefficient of Performance. Figure 6 shows the variation of coefficient of performance with evaporating temperature varies from -6°C to -16°C. It is observed from the figure that the COP of the system decreases when the evaporating temperature decreases. The COP of the system with

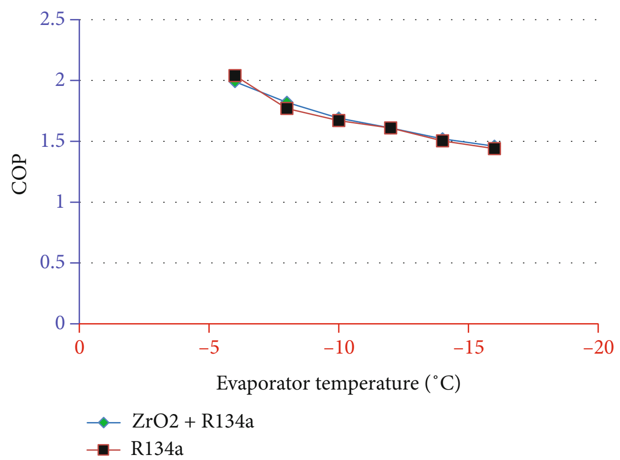

Figure 6: Variation of coefficient of performance for R134a and R134a+ZrO_2.

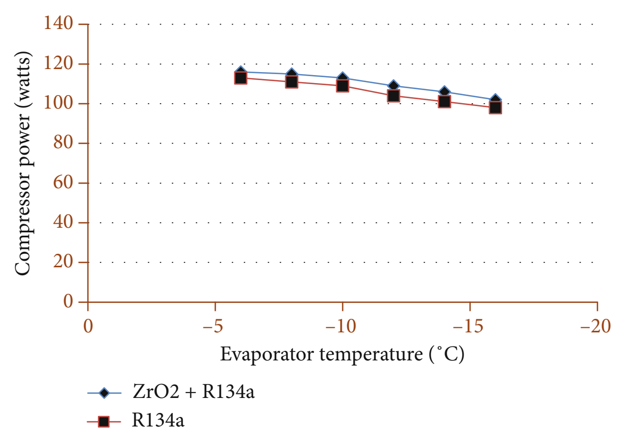

Figure 7: Variation of compressor power for R134a and R134a+ZrO_2.

ZrO_2+R134a nanorefrigerant is higher than that of pure R134a refrigerant.

3.4. Compressor Power. Figure 7 shows the variation of compressor power with evaporating temperature varies from -6°C to -16°C. It is seen from the figure that the compressor power of the system decreases when the evaporating temperature decreases. The compressor takes slightly more power when the system is charged with R134a+ZrO_2 nanorefrigerant.

3.5. Discharge Temperature. Figure 8 shows the variation of discharge temperature with evaporating temperature varies from -6°C to -16°C. It is observed from the figure that the discharge temperature of the system increases when the evaporating temperature decreases. The discharge temperature of the system with ZrO_2+R134a nanorefrigerant is 6.5% lower than that of pure R134a refrigerant.

3.6. Refrigeration Capacity. Figure 9 shows the variation of refrigeration capacity with evaporating temperature varies from -6°C to -16°C. It was seen from the figure the refrigeration capacity of the system decreases when the evaporating temperature decreases. It was observed that the average refrigeration capacity of the system with ZrO_2+R134a

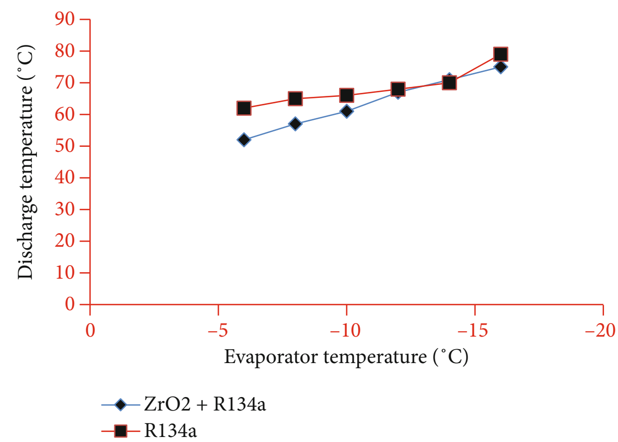

Figure 8: Variation of discharge temperature for R134a and R134a+ZrO_2.

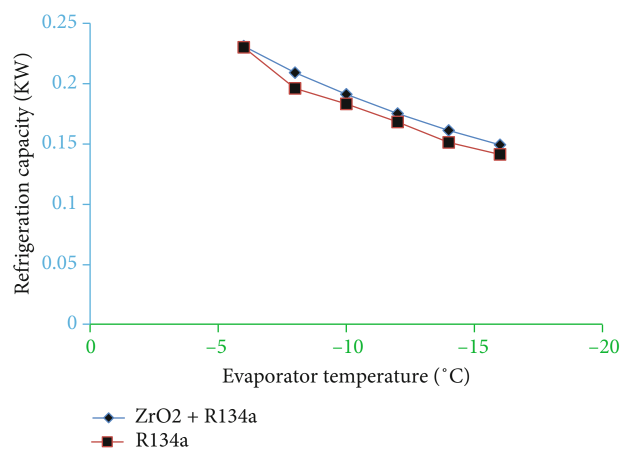

Figure 9: Variation of refrigeration capacity for R134a and R134a+ZrO_2.

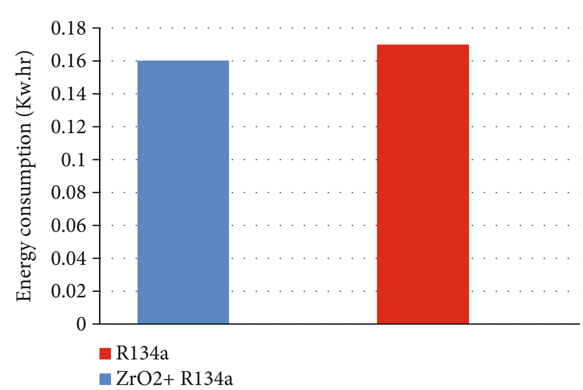

Figure 10: Variation of energy consumption for R134a and R134a+ZrO_2.

nanorefrigerant is 38.70% higher than that of pure R134a refrigerant.

3.7. Energy Consumption. Figure 10 shows the variation of energy consumption for one working cycle with ZrO_2 +R134a nanorefrigerant and pure R134a refrigerant. The energy consumption of the nanorefrigerant was 6.25% lower than that of pure refrigerant.

3.8. Variation of Evaporator Inlet Temperature and Freezer Temperature with Time

4. Conclusion

This experimental work was conducted in the domestic refrigerator with a blend of ZrO_2 nanoparticles in the R134a refrigerant. Based on the experimental calculation, the following specific conclusion could be drawn.

The results indicate that the refrigeration capacity of the system was increased to 38.7% by adding nanoparticles in pure refrigerant using a 0.2 g/L nanoconcentration.

The pull downtime was reduced by 23.53% when using nanorefrigerant at -14°C freezer temperature. It proves that the thermodynamic behaviour of fluid is improved for 0.02%-ZrO_2.

The refrigerator energy consumption is reduced by 6.25% while using nanorefrigerant (ZrO_2+R134a).

The compressor discharge temperature is reduced by 6.5% when the system is charged with R134a+ZrO_2 nanorefrigerant.

The compressor power was slightly increased by adding ZrO_2 nanoparticles to the R134a refrigerant. It has been found that the electricity consumption of the refrigerator was 6.25% lower than that of the base fluid (R134a) when 0.02%-ZrO_2 nanoparticle was added to the system.

Finally, it can be concluded that using nanoparticles in a refrigeration system can improve thermodynamic characteristics and decrease the energy consumption of a domestic refrigerator.

Data Availability

The data used to support the findings of this study are included within the article.

Disclosure

This study was performed as a part of the employment of the authors.

Conflicts of Interest

Authors declare that there are no conflicts of interest.

References

[1] J. C. Maxwell, *A Treatise on Electricity and Magnetism*, Clarendon press, 1873.

[2] S. U. S. Choi and J. A. Eastman*Enhancing thermal conductivity of fluids with nanoparticles*, United States, 1995.

[3] D. Sendil Kumar and R. Elansezhian, “Experimental study on Al2O3-R134a nano refrigerant in refrigeration system,” *International Journal of Modern Engineering Research*, vol. 2, pp. 3927–3929, 2012.

[4] K. Sreejith, “Performance evaluation of a household refrigerator using CuOnano particle lubricant mixture and various other compressor oils with different condenser modes,” *International Journal of Engineering Research and Development*, vol. 5, no. 5, pp. 37–42, 2013.

[5] N. Subramani, A. Mohan, and J. M. Prakash, “Performance studies on a vapour compression refrigeration system using nano-lubricant,” *International Journal of Innovative Research in Science Engineering and Technology*, vol. 2, no. 1, pp. 522–530, 2013.

[6] S. Desai and P. R. Patil, “Application of SiO2 nanoparticles as lubricant additive in VCRS: an experimental investigation,” *Asian Review of Mechanical Engineering*, vol. 4, no. 1, pp. 1–6, 2015.

[7] K. P. Kushwaha, P. Shrivastava, and A. K. Shrivastava, “Experimental study of nano refrigerant (R134a+Al_2O_3) based on vapour compression refrigeration system,” *International Journal Of Mechanical And Production Engineering*, vol. 4, no. 3, 2016.

[8] K. Veera, P. Sreenivasulu Reddy, A. Rizwan Khan, D. Vimal Kumar, and T. Prashanth, “Improvement of COP of vapor compression refrigeration system by using nanorefrigerants,” in *National Conference on Recent Trends & Innovations in Mechanical Engineering*, pp. 172–175, Delhi, India, 2016.

[9] M. E. Haque, R. A. Bakar, K. Kadirgama, M. M. Noor, and M. Shakaib, “Performance of a domestic refrigerator using nanoparticles-based polyolester oil lubricant,” *Journal of Mechanical Engineering and Sciences*, vol. 10, no. 1, pp. 1778–1791, 2016.

[10] V. S. Kumar, A. Baskaran, and K. M. Subaramanian, “A performance study of vapour compression refrigeration system using ZrO_2 nano particle with R134a and R152a,” *International Journal of Scientific and Research Publications*, vol. 6, pp. 410–421, 2016.

[11] B. P. Krishnan, R. Vijayan, and K. Gokulnath, “Performance analysis of a nano refrigerant mixtures in a domestic refrigeration system,” *Advances in Natural and Applied Science*, vol. 11, no. 6, pp. 508–516, 2017.

[12] S. Baskar and L. Karikalan, “Performance study and characteristic on a domestic refrigeration system with additive of zirconium oxide (ZrO_2) nano-particle as nano-lubricant,” *International Journal for Research in Applied Science & Engineering Technology*, vol. 5, no. 10, pp. 1205–1210, 2017.

[13] B. K. Singh and M. S. Ansari, “An experimental study of nanorefrigerant (HC+CuO) based refrigeration system,” *International Journal for Research in Applied Science & Engineering Technology*, vol. 3, pp. 1073–1076, 2017.

[14] G. Jatinder, J. Singh, O. S. Ohunakin, and D. S. Adelekan, “Analyse energetique et exergetique d'un refrigerateur domestique fonctionnant avec du GPL en remplacement du R134a, utilisant du lubrifiant POE et des lubrifiants a base d'huiles minerales TiO_2, SiO_2 et Al_2O_3.,” *International Journal of Refrigeration*, vol. 91, pp. 122–135, 2018.

[15] D. S. Adelekan, O. S. Ohunakin, J. Gill, A. A. Atayero, C. D. Diarra, and E. A. Asuzu, “Experimental performance of a safe charge of LPG refrigerant enhanced with varying concentrations of TiO 2 nano-lubricant in a domestic refrigerator,” *Journal of Thermal Analysis and Calorimetry*, vol. 136, no. 6, pp. 2439–2448, 2019.

[16] A. Baskaran and P. Koshy Mathews, “Energy and exergy analysis of a vapour compression refrigeration system with R134a, R152a and RE170,” *Archives des Sciences*, vol. 66, no. 3, pp. 1–15, 2013.

[17] A. Baskaran and P. K. Mathews, “A performance comparison of vapour compression refrigeration system using eco-friendly refrigerants of low global warming potential,” *International journal of scientific and research publications*, vol. 2, no. 9, pp. 1–8, 2012.

[18] A. Baskaran and P. Koshy Mathews, “A performance comparison of vapour compression refrigeration system using various alternative refrigerants,” *International Journal of Scientific & Engineering Research*, vol. 3, no. 10, 2012.

[19] A. Baskaran and P. K. Mathews, “Thermal analysis of vapour compression refrigeration system with R152a and its blends R429A, R430A, R431A and R435A,” *International Journal of Scientific & Engineering Research*, vol. 3, no. 10, pp. 1–8, 2012.

[20] A. Baskaran and P. K. Mathews, “Comparative study of environment friendly alternatives to R12 and R134a in domestic refrigerators,” *European Journal of Scientific Research*, vol. 92, no. 2, pp. 160–171, 2012.

[21] A. Baskaran and K. Mathews, “Thermodynamic analysis of R152a and dimethylether refrigerant mixtures in refrigeration system,” *Jordan Journal of Mechanical & Industrial Engineering*, vol. 9, no. 4, pp. 289–296, 2015.

[22] A. Baskaran and P. Koshy Mathews, “Investigation of new eco friendly refrigerant mixture alternative to R134a in domestic refrigerator,” *Australian Journal of Basic and Applied Sciences*, vol. 9, no. 5, pp. 297–306, 2015.

[23] A. Baskaran and K. Matthews, “Exergetic analysis of a vapour compression refrigeration system with R134A, RE170, R429A,” *International Journal of Current Advanced Research*, vol. 6, pp. 4029–4036, 2017.

[24] A. Baskaran, N. Manikandan, and V. P. Sureshkumar, “Thermodynamic analysis of di methyl ether and its blends as alternative refrigerants to R134a in a vapour compression refrigeration system,” *International Journal of Advance Engineering and Research Development*, vol. 5, no. 12, 2018.

[25] A. Baskaran, N. Manikandan, and V. P. Sureshkumar, “Effects of sub-cooling on the performance of R152a and Re170 as possible alternatives in a domestic refrigeration system,” *Global Journal For Research Analysis*, vol. 7, no. 11, pp. 289–296, 2018.

[26] Q. Wang, T. Li, Y. Jia, and W. Zhang, “Thermodynamic performance comparison of series and parallel two-stage evaporation vapor compression refrigeration cycle,” *Energy Reports*, vol. 7, pp. 1616–1626, 2021.

[27] A. Baskaran, N. Manikandan, and V. P. Sureshkumar, “Thermodynamic and thermophysical assessment of dimethyl ether and its blends application in household refrigerator,” *International Journal of Scientific Research and Review*, vol. 7, no. 2, 2018.

[28] B. Syed Shaheed, “Performance evaluation of vapour compression refrigeration systems using nano-refrigerants-a review,” *Journal of Advance Research in Dynamical & Control Systems*, vol. 10, p. 5, 2018.

[29] S. Imaduddin, “Performance enhancement of vapour compression system using nano fluid refrigerant,” *International Journal for Research in Applied Science & Engineering Technology*, vol. 6, 2018.

[30] K. S. Pinni, A. S. Katarkar, and S. Bhaumik, “A review on the heat transfer characteristics of nanomaterials suspended with refrigerants in refrigeration systems,” *Materials Today: Proceedings*, vol. 44, pp. 1331–1335, 2021.

[31] S. AFadhilah, R. S. Marhamah, and A. H. M. Izzat, “Copper oxide nanoparticles for advanced refrigerant thermophysical properties: mathematical modelling,” *Journal of Nanoparticles*, vol. 2014, 5 pages, 2014.

[32] T. Coumaressin and K. Palaniradja, “Performance analysis of a refrigeration system using nano fluid,” *International Journal of Advanced Mechanical Engineering*, vol. 4, pp. 459–470, 2014.

[33] S. S. Sanukrishna, A. S. Vishnu, and M. Jose Prakash, “Nanorefrigerants for energy efficient refrigeration systems,” *Journal of Mechanical Science and Technology*, vol. 31, no. 8, pp. 3993–4001, 2017.

[34] D. S. Kumar and R. Elansezhian, “ZnO nanorefrigerant in R152a refrigeration system for energy conservation and green environment,” *Frontiers of Mechanical Engineering*, vol. 9, no. 1, pp. 75–80, 2014.

[35] S. Özerinç, S. Kakaç, and A. G. Yazıcıoğlu, “Enhanced thermal conductivity of nanofluids: a state-of-the-art review,” *Microfluidics and Nanofluidics*, vol. 8, no. 2, pp. 145–170, 2010.

[36] T. A. A. Broadbent, “Investigations on the Theory of the Brownian Movement,” in *A EinsteinThe Principles of Mechanics, Hydrodynamics*, The Mathematical Gazette, H. Hertz, H. L. Dryden, F. P. Murnaghan, and H. Bateman, Eds., Dover Publications, New York, 1957.

[37] H. C. Brinkman, “The viscosity of concentrated suspensions and solutions,” *The Journal of Chemical Physics*, vol. 20, no. 4, pp. 571–571, 1952.

[38] G. K. Batchelor, “The effect of Brownian motion on the bulk stress in a suspension of spherical particles,” *Journal of Fluid Mechanics*, vol. 83, no. 1, pp. 97–117, 1977.

[39] B. C. Pak and Y. I. Cho, “Hydrodynamic and heat transfer study of dispersed fluids with submicron metallic oxide particles,” *Experimental Heat Transfer an International Journal*, vol. 11, no. 2, pp. 151–170, 1998.

[40] Y. Xuan and W. Roetzel, “Conceptions for heat transfer correlation of nanofluids,” *International Journal of Heat and Mass Transfer*, vol. 43, no. 19, pp. 3701–3707, 2000.